AN ALN TWO-DIMENSIONAL ACOUSTIC WAVE HUMIDITY SENSOR WITH GRAPHENE OXIDE AS SENSING LAYER

Xianhao Le and Jin Xie
State Key Laboratory of Fluid Power and Mechatronic Systems, Zhejiang University, Hangzhou 310027, People's Republic of China

ABSTRACT

In this paper, we firstly report an AlN thin film two-dimensional acoustic wave humidity sensor with graphene oxide (GO) as sensing layer. The sensor with small sensing area show high sensitivity up to 218.6 kHz/10%RH with a wide detection range from 10% to 90%RH. The sensor has excellent performance in terms of repeatability and stability. Little hysteresis, fast response and short recovery time of the sensors are obtained. The TCF of the sensor is about -15.8 ppm/^{o}C, much smaller than conventional humidity sensors.

INTRODUCTION

Humidity sensors have received much attention in recent years due to their wide application in people's daily life, industry process control and agriculture [1-2]. Vary types of humidity sensors based on different working principles have been developed to meet people's needs, such as surface acoustic wave (SAW) humidity sensors [3], capacitive humidity sensors [4], optical humidity sensors [5], and so on. So far, humidity sensors still have some problems like large size, long response and recovery times, narrow testing range, instability and easily affected by temperature variation during the humidity detecting process.

In order to acquire higher sensitivities, different types of sensitive membranes are deposited on the surface of the sensors. Graphene oxide (GO) as a graphene derivative shows an excellent humidity sensing ability duo to its large surface-to-volume ratio and high hydrophilicity [6]. Unlike graphene, the GO film is electrically insulating because of its chemical groups, which makes it useful in SAW and capacitive humidity sensors. Recently, GO thin film coated humidity sensors have proved to have high sensitivity, fast response and recovery time [7-9].

This paper investigates the relative humidity detection by utilizing a novel GO thin film coated two-dimensional acoustic wave humidity sensor. The sensor uses the checker-patterned electrodes to excite two-dimensional acoustic wave simultaneously [10]. The sensor can operate at both quasi-symmetrical (QS) mode and quasi-asymmetric (QA) mode like the traditional lamb wave resonators. Sensing performances of the sensor with various surface treatments (both the top surface and bottom surface), operating modes and different electrode configurations are studied respectively. The humidity sensitivity of the sensor can be improved by coating with a thicker GO film, utilizing higher order mode and adopting a grounded bottom electrode. Comparable sensitivity (218.6 kHz/10%RH) of the sensor has been measured with a small sensing area (316×316 μm2). The sensor shows little hysteresis, excellent repeatability and stability with a wide detection range from 10% to 90%RH. Both fast response (12s) and short recovery time (6s) of the sensor are obtained if we test the resonant frequency during absorption process and test the insert loss during desorption process. Unlike the conventional humidity sensors, the sensor studied in this work has a small TCF about -15.8 ppm/ ^{o}C.

EXPERIMENTAL

Sensor design and fabrication

The structure of the two-dimensional acoustic wave humidity sensor is illustrated in Figure 1. Checker-patterned electrodes are placed on the thin AlN film to excite two-dimensional plate acoustic waves and the free edge reflector is adopted to reduce the acoustic loss. The checker-patterned electrodes consist of 12 square-shaped electrodes. Each square-shaped electrode shares the same length of 56 um and the wavelengths of the device in both direction are 59 μm. Surfaces (both the top surface and bottom surface) of the sensor are covered with various GO thin films, sensing area of each face of the sensor is about 316×316 μm^2.

A commercially available multi-user MEMS process (PiezoMUMPs) was used to fabricate the sensors, which mainly consists of a thin AlN layer (0.5μm) and a thick low damping Si layer (10μm), the upper surface of the Si layer is highly-doped to act as the bottom electrode. This kind of thin-film piezoelectric-on-silicon (TPOS) devices using highly-doped Si layer have proved to have high electromechanical coupling, low loss [11] and very good performance for temperature compensation [12]. The SEM image of the fabricated two-dimensional acoustic wave sensor is shown in Figure 2(a).

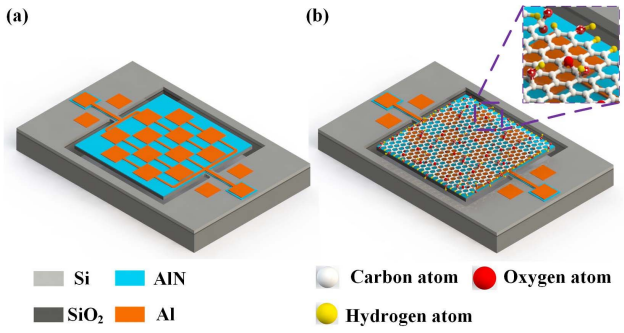

Figure 1: Schematics of the two-dimensional acoustic wave sensors (a) with clean surface and (b) covered with GO layer.

Deposition of graphene oxide sensing layer

In order to avoid forming a significant non-uniformity thickness of GO layer on the surface of the sensor. The initial GO dispersion with a concentration of 4.6 mg/ml was diluted by deionized (DI) water to form the GO dispersions with concentrations of 0.23 and 0.46 mg/ml. Then the GO dispersions with different concentrations

were dropped over the surface of the sensors through a microliter syringe to form different thickness GO layers.

Figures 2(b) and (c) show the SEM pictures of the surface of the sensor before and after GO film coating. Typical S_{21} transmission curves of the humidity sensors with and without GO layer at the same relative humidity are reported in Figure 2(d). The resonant frequency of GO coated sensor decreases slightly due to the mass loading effect caused by GO layer, but the insertion loss and spurious mode are also reduced because of the GO film.

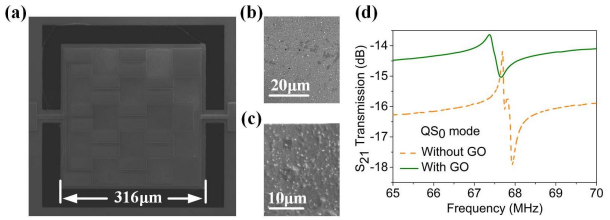

Figure 2: SEM images of the device (a), and its surface before (b) and after (c) coating with GO film. (d) Transmission spectrum of the sensor before and after GO coating.

Two-dimension acoustic wave humidity sensors (both at top surface and bottom surface) coated with various thickness of GO layers were fabricated for humidity sensing. Three samples (D1, D2, D3) were selected from the manufactured sensors, specific parameters and characteristics of the samples are listed in Table 1. The sensing performance of the sensor utilizing different modes was also investigated.

Table 1.Summary of the parameters and characteristics of the sensors.

Sample	Mode	Frequency (MHz)	GO thickness (nm)	
			Top surface	Bottom surface
D1	QS_0	67.69	100-150	0
D2	QA_0	13.78	200-300	0
	QA_1	46.61		
	QS_0	67.52		
	QA_2	81.45		
	QS_2	217.47		
D3	QS_0	67.55	100-150	200-300

Humidity sensing

A metallic chamber with a volume of about 86 cm^3 was designed to create a relatively sealed environment, the humidity sensor was fixed in the chamber as described in Figure 3. The relative humidity in the chamber was precisely changed by manually adjusting the flow ratio of dry and wet N_2 gas. A commercial hygrothermograph was connected to the chamber to detect the relative humidity in the chamber real-timely. Transmission properties of the humidity sensor were investigated using a network analyzer (Agilent E5061B). In order to investigate the repeatability and response time of the humidity sensor, we developed a LabVIEW (National Instruments) based program to automatically record the parameters change with the time during cyclic change in relative humidity. All the experiments were conducted at 23±0.5 °C.

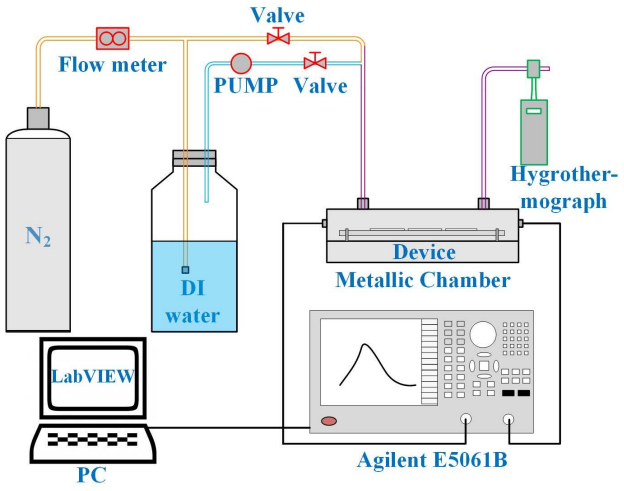

Figure 3: Diagram of the experimental setup for humidity sensing.

RESULTS AND DISCUSSION

Sensitivities of the humidity sensors with different surface treatments are firstly studied. The humidity sensitivity S is defined as follows:

$$S = \frac{\Delta f}{\Delta RH} \quad (1)$$

where the Δf and ΔRH represent the frequency shift and relative humidity change respectively. Figure 4(a) reports the resonant frequency shift of the three samples as a function of relative humidity, the samples work at QS_0 modes and the relative humidity is manually changed from 10% to 90%RH at intervals of 10%RH. Thicker GO films have stronger ability of water molecules adsorption. The resonant frequency shift of the sensor is mainly caused by mass loading effect, hence sensor with thicker GO layer has higher sensitivity, as revealed by comparing the sensing performances of samples D1 and D2. According to the test results of samples D1 and D3, the GO layer on the top surface of the sensor improves sensitivity more significantly than the GO layer on the bottom surface. This is because the acoustic wave energy mainly confined in the AlN layer, the top surface of the sensor is more sensitive to surface perturbation. The sample D2 is chosen to have an in-depth investigation, as it has higher sensitivity.

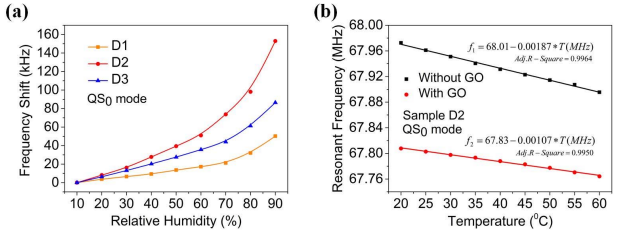

Figure 4: (a) Resonant frequency shift as a function of relative humidity for the QS_0 mode of samples D1, D2 and D3 respectively. (b) Measured resonant frequency variations versus temperature of the sample D2 with and without GO layer.

During the humidity sensing process, temperature

change also will causes the frequency shift of the sensor. Resonant frequency of the sensor has a very good linear relationship with temperature as shown in Figure 4(b), the definition of temperature coefficient of frequency (TCF) is

$$\mathrm{TCF}=\frac{1}{f}\frac{\Delta f}{\Delta T} \qquad (2)$$

where f and ΔT are resonant frequency and temperature change respectively. The TCF of the sample D2 without GO layer is -27.5 ppm/°C. With GO layer covering on the top surface, the Sample D2 has a lower TCF of -15.8 ppm/°C much smaller than conventional SAW humidity sensors.

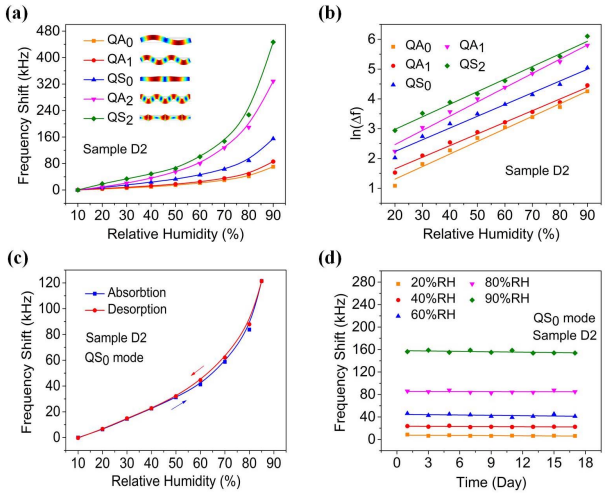

Figure 5: (a) Resonant frequency shift as a function of the relative humidity for QA_0, QA_1, QS_0, QA_2 and QS_2 modes of sample D2. (b) Resonant frequency shift as an exponential function of the relative humidity for each modes of sample D2. Humidity hysteresis characteristic (c) and stability (d) of sample D2.

Figure 5(a) compares the sensing performances of sample D2 operating from QA_0 to QS_2 modes. Resonant frequencies of the modes various from 14.79 to 217.47 MHz. The higher frequency mode the sensor utilizes during humidity sensing process, the higher sensitivity the sensor will have, and the sensitivity of the sensor is up to 218.6 kHz/10%RH at 90% RH utilizing QS_2 mode. The sensitivities of each mode of the sensor at 90%RH are summarized in Table 2. Logarithmic function of frequency shifts have an excellent linearity (0.9821<R2<0.9906) for each mode of sample D2 as presented in Figure 5(b). Frequency shift and relative humidity approximately have an exponential relationship.

Table 2: Summary of sensitivities of each mode of sample D2 at 90%RH.

Mode	QA_0	QA_1	QS_0	QA_2	QS_2
Sensitivity kHz/10%RH	28.9	37.3	74.5	142.5	218.6

Large hysteresis and instability performance of sensor restrict its practical application. As shown in Figure 5(c), the sensor in this paper has a little hysteresis as the relative humidity is changed from 10% to 85%RH and then back to 10%RH. In order to investigate the stability of the sensor, the sensor is tested repeatedly at fixed relative humidity of 20%, 40%, 60%, 80% and 90%RH in a period of 17 days. The test data presented in Figure 5(d) show a good consistency and the frequency variation is less than 5% at each relative humidity level.

Short-term repeatability of sample D2 is studied through a cyclic change of relative humidity from 20% to 80%RH. As shown in Figures 6(a) and (b), both the resonant frequency and insertion loss of the sensor have a good repeatability with a three times cyclic change of relative humidity. Figures 6(c) and (d) reveal the details of the response and recovery behaviors of the sensor by measuring resonant frequency and insert loss to relative humidity change. The time interval between each two data points is set to 1.5 seconds. The timing begin with the relative humidity change and end with the values of resonant frequency and insert loss reach 96% of the final values. The response and recovery time for resonant frequency change are 12 and 21 seconds, response process is faster than recovery process, and for insert loss change, the response and recovery time are 31 and 6 seconds, recovery process is faster than response process. The sensor will have both fast response and recovery speeds, if we test resonant frequency during absorption process and test insert loss during desorption process.

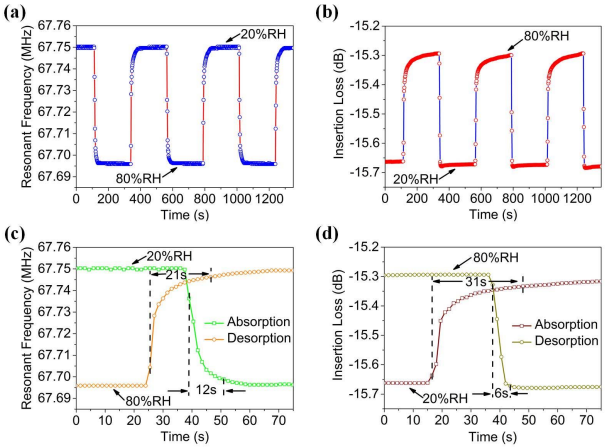

Figure 6: Response of resonant frequency (a) and insertion loss (b) of sample D2 to relative humidity, when the humidity is repeatedly changed from 20% to 80%RH. Response and recovery times of resonant frequency (c) and insertion loss (d) of the device.

Lamb wave resonators with different electrode configurations (bottom electrode floating and grounded) have different characteristics [13]. Similar to the conventional lamb wave resonators, electrode configurations of the two-dimensional acoustic wave sensors also have impacts both on the characteristics of the sensors and the sensors' performances during humidity sensing process. Figure 7(a) shows a comparison of S_{21} response in QA_0 mode of two-dimensional acoustic wave sensors with different configurations of bottom electrodes. The sensor with grounded bottom electrode has a lower insert loss and higher sensitivity than the one with floating electrode. As shown in Figure 7(b), utilizing grounded bottom electrode, the average sensitivities (at 90%RH) of

the sensor increase from 8.78 to 13.05 kHz/10%RH for QA_0 mode and from 19.11 to 40.51 kHz/10%RH for QS_0 mode.

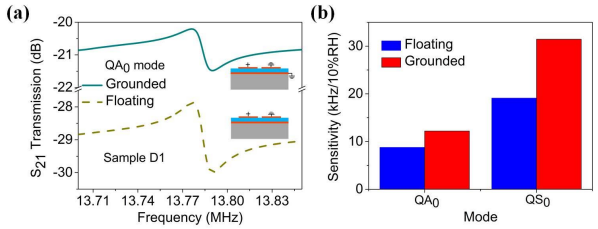

Figure 7: S_{21} transmission plots (a) and sensitivity comparison (b) of the sensors with different bottom electrode configurations.

CONCLUSION

In this study, we proposed an AlN two-dimensional acoustic wave humidity sensor with graphene oxide as sensing layer. Experimental results show the sensor's humidity sensitivity increases as the thickness of GO film increases, and the top surface of the sensor is more sensitive to humidity change compare with the bottom surface. The sensor can also obtains higher sensitivity by utilizing the mode with high resonant frequency. When the sensor operates at QS_2 mode, the humidity sensitivity of the sensor reaches up to 218.6 kHz/10%RH at 90%RH. The sensor has wide detection range from 10% to 90%RH with little hysteresis, and have excellent performance in terms of repeatability and stability. Both fast response (12s) and short recovery time (6s) of the sensor are obtained by testing the resonant frequency during absorption process and testing the insert loss during desorption process. The TCF of the sensor is about -15.8 ppm/^{o}C much smaller than conventional SAW humidity sensors. In addition, with a grounded bottom, the sensitivity of the sensor can be further improved.

ACKNOWLEDGEMENTS

This work is supported by the "National Natural Science Foundation of China (51475423)", the "Zhejiang Provincial Natural Science Foundation of China (LY14E050018)" and the "Science Fund of Creative Research Groups of National Natural Science Foundation of China (51521064)".

REFERENCES

[1] C. Y. Lee and G. B. Lee, "Humidity sensor: a review", *Sensor Letters*, vol. 3, pp. 1-14, 2005.

[2] H. Farahani, R. Wagiran and M. N. Hamidon, "Humidity sensors principle, mechanism, and fabrication technologies: a comprehensive review", *Sensors*, vol. 14, pp.7881-7939, 2014.

[3] D. J. Li, C. Zhao, Y. Q. Fu and J. K. Luo, "Engineering silver nanostructures for surface acoustic wave humidity sensors sensitivity enhancement", *Journal of Electrochemical society*, vol. 161, pp. 151-156, 2014.

[4] W. C. Wang, Y. T. Tian, K. Li, E. Y. Lu, D. S. Gong, and X. J. Li, "Capacitive humidity-sensing properties of Zn_2SiO_4 film grown on silicon nanoporous pillar array", *Applied Surface Science*, vol. 273, pp. 372-376, 2013.

[5] S. Muto, O. Suzuki, T. Amano and M. Morisawa, "A plastic optical fibre sensor for real-time humidity monitoring", *Measurement Science and Technology*, vol. 12, pp. 746-750, 2003.

[6] F. Barroso-Bujans, S. Cerveny, A. Alegria, and J. Colmenero, "Sorption and desorption behavior of water and organic solvents from graphite oxide", *Carbon*, vol. 48, pp. 3277-3286, 2010

[7] H. C. Bi, K. B. Yin, X. Xie, J. Ji, S. Wan, L. T. Sun, M. Terrones and M. S. Dresselhaus, "Ultrahigh humidity sensitivity of graphene oxide", *Scientific reports*, vol. 3, 2013.

[8] W. P. Xuan, M. He, N. Meng, X. L. He, W. B. Wang, J. K. Chen, T. J. Shi, T. Hasan, Z. Xu, Y. Xu and J. K. Luo, "Fast response and high sensitivity ZnO/glass surface acoustic wave humidity sensors using graphene oxide sensing layer", *Scientific reports*, vol. 4, 2014.

[9] Y. Yao, X. D. Chen, H. H. Guo, Z. Q. Wu and X. Y. Li, "Humidity sensing behaviors of graphene oxide-silicon bi-layer flexible structure", *Sensor and Actuators B: Chemical*, vol. 161, pp. 1053-1058, 2012.

[10] L. Khine, J. B. W. Soon and J. M. Tsai, "Piezoelectric AlN MEMS resonators with high coupling coefficient", in *Transducers'11*, Beijing, June 5-9, 2011, pp. 526-529.

[11] R. Abdolvand, H. M. Lavasani, G. K. Ho and F. Ayazi, "Thin-film piezoelectric-on-silicon resonators for high-frequency reference oscillator applications", *IEEE transactions on ultrasonics, ferroelectrics, and frequency control*, vol. 55, pp. 2596-2606, 2008.

[12] M. Shahmohammadi, B. P. Harrington, R. Abdolvand, "Zero temperature coefficient of frequency in extensional-mode highly doped silicon micro-resonators", in *IEEE International Frequency Control Symposium Proceedings*, 2012, pp. 1-4.

[13] C. M. Lin, V. Yantchev, J. Zou, Y. Y. Chen, and A. P. Pisano, "Micromachined one-port aluminum nitride Lamb wave resonators ultilizing the lowest-order symmetric mode", *Journal of microelectromechanical systems*, vol. 23, pp. 78-91, 2014.

CONTACT

*Jin Xie, tel: +86-571-87952274; xiejin@zju.edu.cn